AJ ACADEMIC JOURNALS
expand your knowledge

Journal of Petroleum and Gas Engineering

Full Length Research Paper

Influence of wavelet phase rotation on post stack model based seismic inversion: A case study of X-field, Niger Delta, Nigeria

Aniefiok Sylvester Akpan[1], Daniel N. Obiora[1]*, Francisca N. Okeke[1], Johnson C. Ibuot[1] and Nyakno J. George[2]

[1]Department of Physics and Astronomy, University of Nigeria, Nsukka, Enugu State, Nigeria.
[2]Department of Physics, Akwa Ibom State University, Ikot Akpaden, P. M. B. 1169, Uyo, Akwa Ibom State, Nigeria.

The effect of wavelet phase rotation on post inversion in X-field Niger Delta has been investigated. This paper demonstrates the influence of wavelet phase employed in model based seismic inversion. It presents the problem associated with variation in wavelet phases employed in post-stack model based seismic inversion which affect the discrimination of litho-fluid contrast from inverted seismic volume. The study was carried out using 3D post stack seismic data and well logs from three (3) exploratory wells in the study area. The data was inverted into acoustic impedance (P–impedance) using five different wavelets with 0, 15, 30, 45 and 60° phases for each inversion process. The inverted P-impedance slices result for the different wavelet phases were compared and the effect of each wavelet on the inverted section was deciphered. Small decrease in impedance error was observed for zero degree (0°) and minimum (15 to 30°) wavelet phase. Alternatively, inverted P–impedance section using 45 and 60° wavelets phase depict high error in the impedance and less correlation coefficient with increase in the synthetic error. This study thus recommends zero degree (0°) or minimum phase (15 to 30°) wavelets for interpretation in the study area as the degree of variation in input wavelet greatly affects the inverted acoustic impedance results.

Key words: Niger Delta, wavelet, well logs, seismic data, stack inversion.

INTRODUCTION

The ultimate goal of seismic inversion is the prediction of rock and fluid properties for the characterization of hydrocarbon reservoirs using seismic data. Seismic inversion provides the most detailed view of the subsurface and because of this efficiency; inversion method is employed by oil and gas companies to

increase the resolution and reliability of seismic data to improve the estimation of rock properties such as porosity and net pay. This, according to Maurya and Sarkar (2016) enable extraction of the underlying physical characteristics of rocks and fluids from seismic and well log data. Seismic inversion otherwise referred

*Corresponding author. E-mail: daniel.obiora@unn.edu.ng.

Figure 1. Location map of the study area.

to as stratigraphic deconvolution attempts to put a spiked response at geological boundaries (lithologic changes) and the main reservoir characteristic interface (Veeken and Rauch-Davies, 2006). The application of seismic inversion in reservoir characterization has over the years led to various advancements in the technique. These advancements include the development of several inversion methods which industries utilized for the prediction of rock and fluid properties from either post stack or pre-stack time migrated seismic data. There are several seismic inversion methods such as; amplitude fluid inversion (AFI) and time lapse (4D seismic) inversion (Gluck et al., 2000; Oldenziel, 2003; Alaminiokuma and Ofuyah, 2017). These techniques depend on a number of parameters such as low frequency model, wavelet phase, wavelength of the wavelet and frequency of wavelet. These parameters are employed in building an acoustic impedance attribute model that is inverted in an attempt to extract the geologic response of the earth which causes the seismic event in the area under study. The acoustic impedance attribute is gradually replacing the normal amplitude seismic representation as inversion is becoming an integral part of reservoir characterization workflow (Latimer et al., 2000; Van-Riel, 2000). In the industries today, seismic inversion is a routine processing step in field development studies as well as exploration purposes.

Generally, different types of inversion start with different types of traces with the main distinction among them being between inversion performed before stacking (pre-stack) and inversion after stacking (post-stack). The first approach of seismic inversion is the most commonly used inversion analysis in which the effect of the wavelet is removed from the seismic data and a high resolution

image of the subsurface is produced (Margrave et al., 1998). The second approach of seismic inversion relies on model building using well log, seismic and geological data (Downtown, 2005). Post stack seismic inversion on which this study is based employs the estimation of rock physical properties by combining seismic and well log data with the physical parameters such as impedance, velocity and density.

Since seismic inversion depends mostly on the wavelet, it therefore implies that obtaining a good inversion result lies wholly on selection of a good wavelet phase. In this study, an attempt is made to investigate the influence of variation in wavelet phase in inverting the same geologic model in X-field, Niger Delta (Figure 1).

Geology of Niger Delta

Niger Delta is a major hydrocarbon producing basin in Nigeria where intensive exploration and exploitation activities have been on, since early 1960's owing to the discovery of commercial oil in Oloibiri-1 well in 1956 (Reijers, 1996; Ajaegwu et al., 2012). The Basin is regarded as Africa's leading province in recent times. Niger Delta is covered with a dense grid of 2D and 3D seismic data penetrated by over 5,000 wells. The Basin is situated in the apex of the Gulf of Guinea on the West Coast of Africa. The Basin was formed by the buildup of sediments over a crustal tract developed by faulting during the Precambrian with outlines controlled by deep seated faults associated with rifting (Weber and Daukoru, 1975).

The tertiary section of Niger Delta is divided into three distinct lithofacies in ascending order as shown in Figure 2
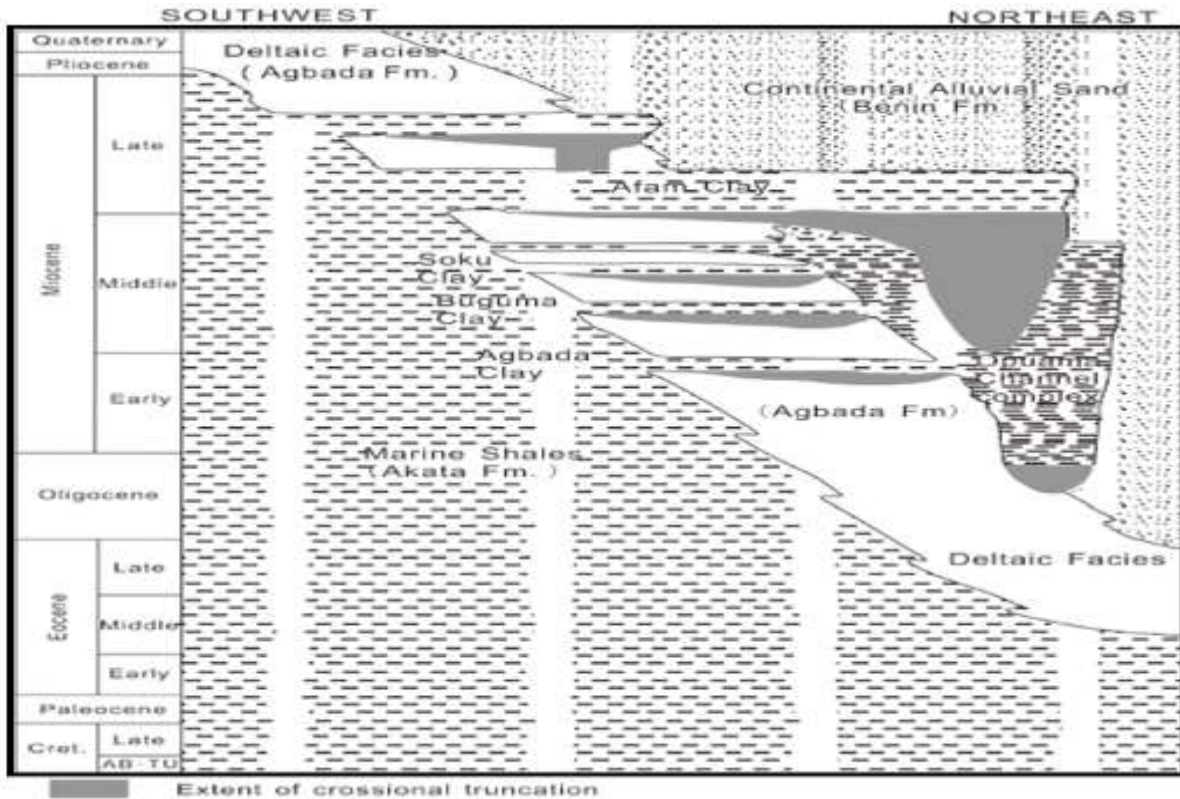
Figure 2. Stratigraphic succession map of Niger Delta.
Source: Doust and Omatsola (1990).

Akata, Agbada and Benin Formations, respectively (Short and Stauble, 1967). Akata Formation being the potential source rock is estimated to be up to 7000 m thick while Agbada and Benin Formations are estimated to be 3700 m and 2000 m thick, respectively (Michele et al., 1999). The Akata formation consists of clays and shales with minor sand intercalations. The sediments were deposited in prodelta environment. The sand percentage here is generally less than 30% (Nuhu, 2009). This formation at the base of the delta is of marine origin and is composed of thick, dark grey shale sequence (potential source rock), turbidite sands (potential reservoirs) (Weber and Daukoro, 1975). The Agbada formation consists of alternating sand and shales representing sediments of the transitional environment comprising the lower delta plain (mangrove swamps, floodplain, marsh) and the coastal barrier and fluviomarine realms. The sand percentage within the Agbada formation varies from 30 to 70%, which results from the large number of the depositional off lap cycles (Nuhu, 2009). The Benin formation consists of high sand percentage (30 to 70% and forms the top layer of the Niger Delta depositional sequence (Nuhu, 2009). The Benin formation comprises the top part of the Niger Delta clastic wedge and consists mainly of sands and gravels which extend to depth of about 2000 m. It extends from the Benin-Onitsha area in the north to beyond the present Coastline (Doust and Omatsola, 1990).

Theory of seismic method

Seismic trace occurs as a result of the convolution of the earth's reflectivity $R(t)$ with wavelet $W(t)$ plus noise $N(t)$. Hence seismic trace $S(t)$ is given by Equation 1 as:

$$S(t) = R(t) * W(t) + N(t) \qquad (1)$$

where * is the convolution.
   Assuming that the noise component is negligible during processing, Equation 1 then reduces to:

$$S(t) = R(t) * W(t) \qquad (2)$$

Since working in frequency domain is more preferable to the time domain, a problem arises when Equation 2 is converted into frequency domain. The lowest and highest frequencies tend to be missing as a result of the band limited nature of the seismic data. The lower frequencies
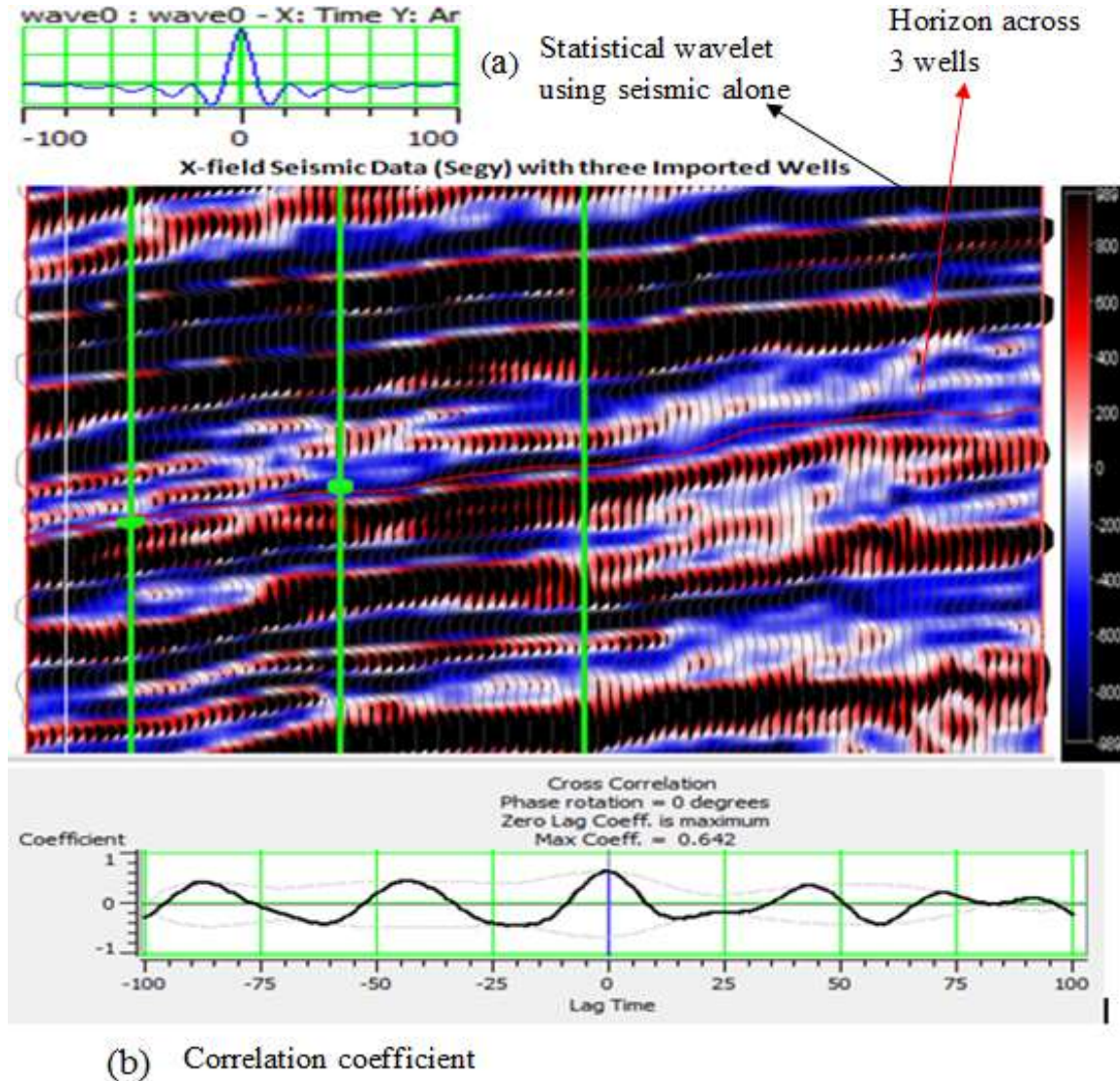
Figure 3. (a) Statistical wavelet and seismic data with Horizon (red) across the 3 imported wells (green), and (b) cross correlation window showing re-corrected wavelet coefficient of 0.642.

are most critical to rock properties as it leads to determining fluid, porosity and all other reservoir properties required to take a drilling decision. Therefore, a low frequency trend model is necessary in order to really find out what is going on beneath the earth (Chirag, 2013).

METHODOLOGY

The study was carried out using 3D post stack seismic data and suites of well logs from three (3) exploratory wells in the field. The well log data comprises gamma ray, resistivity, formation density, caliper and spontaneous potential logs. These logs were median filtered using an operator length of six to correct borehole irregularities encountered during drilling which can introduce spikes/unwanted signals in the recorded well log data. Checkshot

correction was applied to the sonic derived P-wave log estimated using the sonic log transit time relation given in Equation 3.

$$\Delta t_{\log} = \frac{1}{V_P} \quad (3)$$

where, V_P is the sonic derived P-wave velocity and $\Delta t_{\log}$ is the sonic transit time.

Statistical wavelet with zero phase shown in Figure 3 was extracted from the seismic volume. The extracted wavelet was used for seismic to well correlation. A correlation coefficient of less than 15% and a wavelet with a constant phase of (-69°) was estimated. The estimated wavelet phase was rotated to zero phase through the addition of (+69°). This was achieved using the wavelet phase rotation mathematical relation given in Equation 4. The rotated zero phase wavelet was employed in correlating the seismic and well log data. The seismic to well tie correlation gives a significant
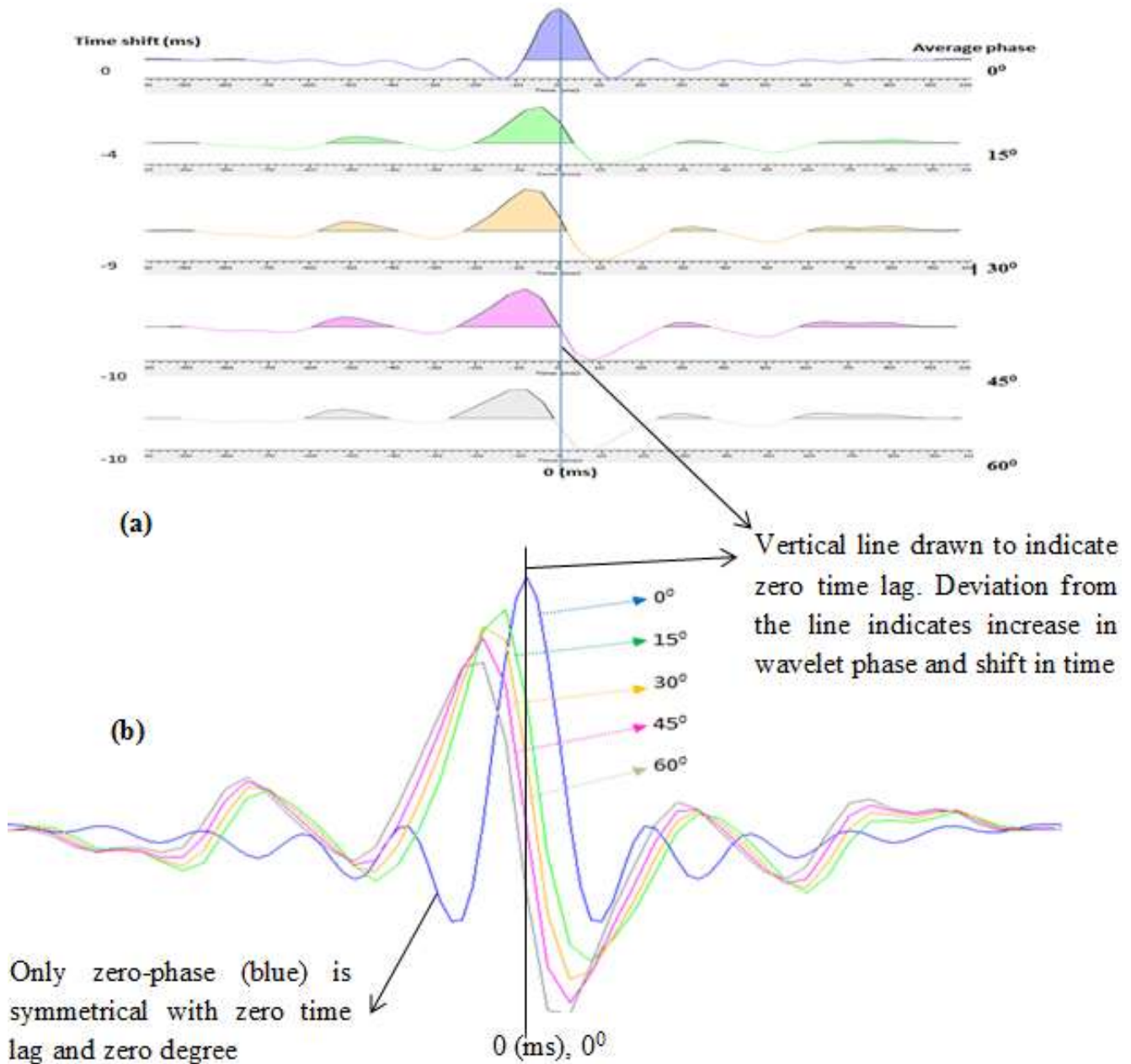
Figure 4. (a) A rotated phase of re-corrected wavelet from 0^0 - 60^0 by a constant of 15^0 interval using Equation 2, (b) Stacking of amplitude spectra for all rotated wavelets to examine their symmetrical nature.

improvement in the correlation coefficient which increased from 15 to 64% as shown in Figure 3.

$$W(n) = R + n + K \tag{4}$$

Where $n = 0^0$, 15^0, 30^0, 45^0 and 60^0, $R = 69$ is the corrected phase constant, $K = -69$ is the extracted phase constant, and $W(n)$ is the rotated wavelet phase.

The extracted wavelet phase was varied with a constant of 15° to generate subsequent wavelet phases using Equation 4. The amplitude/phase spectra of each rotated wavelet phase were examined and their corresponding shift in time determined as

shown in Figure 4. Values were substituted for the constants R, n and K to estimate the wavelet phases given in Equations 5 to 7.

$$W(0) = 69 + 0 + (-69) = 0° \tag{5}$$

$$W(15) = 69 + 15 + (-69) = 15° \tag{6}$$

$$W(30) = 69 + 30 + (-69) = 30°, \text{ etc} \tag{7}$$

One horizon (red line) was picked across the seismic volume which served as geologic framework for the model building. The initial P-impedance model (Figure 5) was built using the recorrected zero phase wavelet and horizon with three wells. A processing time
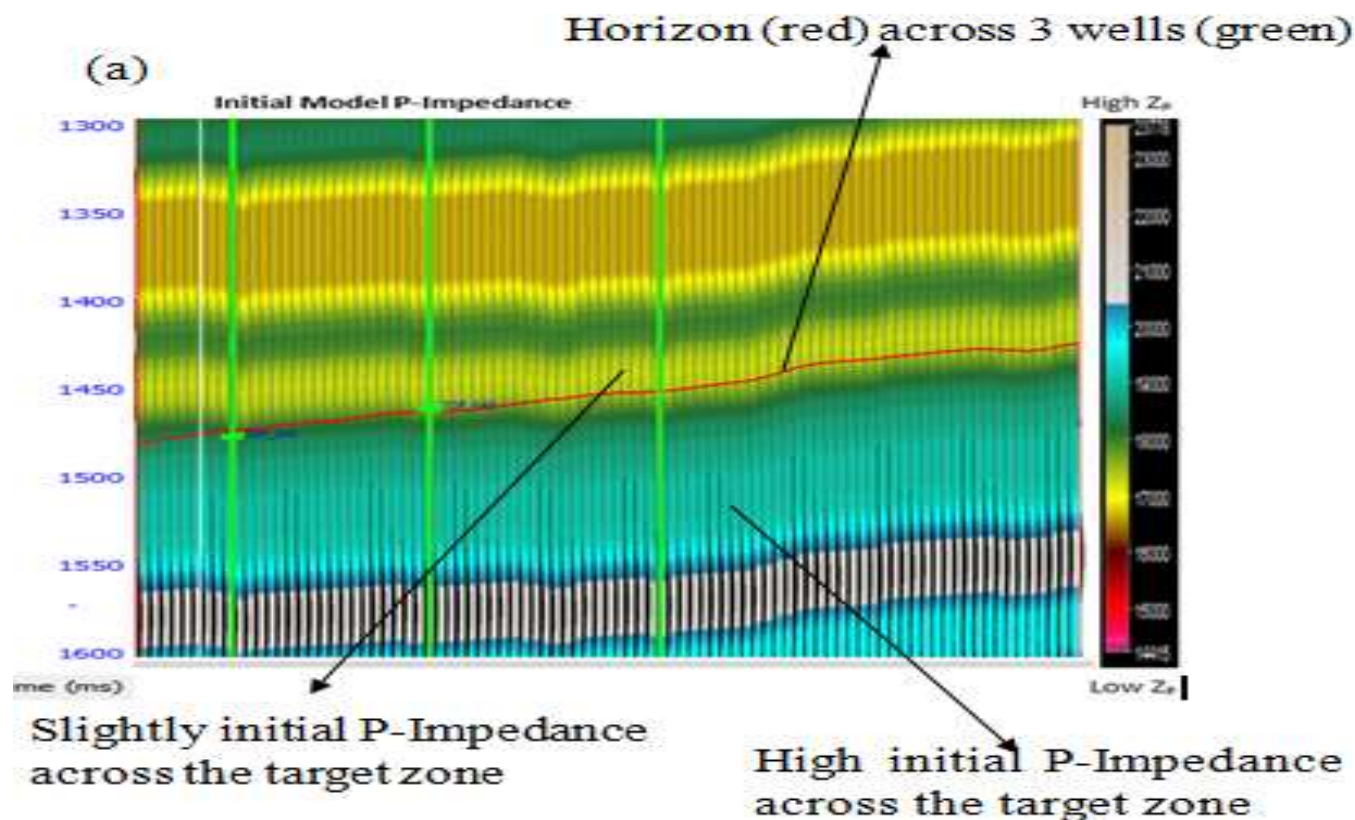
Figure 5. 3D view of initial impedance with picked horizon across the top of reservoir of the three wells imported.

window of 1300 to 1600 ms was selected for the inversion to avoid overshadowing the prospective reservoir zones by noisy areas while hard constraint was chosen to limit the amount of deviation from the inserted volume. Quality control measures were taken for each step to ascertain the accuracy of the P-impedance slices generated. The created P-impedance model was inverted separately using the rotated wavelet phases of *15, 30, 45* and *60⁰* obtained through phase rotation. Hard constraint option was chosen to limit the rate of deviation of the inverted volume from the initial model. An average block size of 4 ms, 10 number of iterations and 1% prewhitening were inversion parameters chosen to limit the amount of noise in the data.

RESULTS

The inversion analysis results with varying wavelet phases and the corresponding impedance error for each inverted volume are shown in Figures 6(a, b, c), 7(a, b, c), and 8(a, b), respectively. These results depict the effect of wavelet phase rotation on the inverted seismic sections. Figure 6(a) and (b) show the inversion analysis windows for 0° and 45° wavelet phases between a time window ranging from 1300 – 1600 ms of inverted acoustic impedance crossections. The results reveal the differences in impedance distribution across the volumes. These differences are observed within the target window of the Zp in red superimposed with initial model in black,

P-wave log in blue and the Zp error in black colour, a generated synthetic in red wiggles, seismic trace in black wiggles and correlation error traces in red wiggles. The summary of the variations in these parameters are shown in Table 1 which indicate the differences in Zp occuring as a result of variation in wavelets phases on post stack inversion.

Table 1 shows Zp error, correlation coefficient and synthetic error for the wavelet phase employed in each inversion process. From Table 1, an increase is observed in Zp error of 1734.63 and 1941.83 for 0 and 45° wavelet phases respectively. This indicate a 5% increase in Zp error relative to 0° Zp error. Also, correlation coefficients of 0.996523 and 0.996347 are deciphered for the two wavelet phases (0° and 45°) while the synthetic error increased by 2% when compared to the 0° wavelet phase as shown in Figure 6(a, b).

Figure 7(a), (b) and (c) show the inverted P-impedance section for 0, 15 and 30° wavelet phase from a time window range of 1300 to 1600 ms. The section depicts the picked horizon which spread across the reservoir top and the three (3) exploratory wells in the field. A good match is observed between the I$_P$ features distribution. The low and high impedance zones agree to some extent with the reservoir tops from the horizon. At the reservoir top, around a time window of 1500 ms, the lowest I$_P$ values of
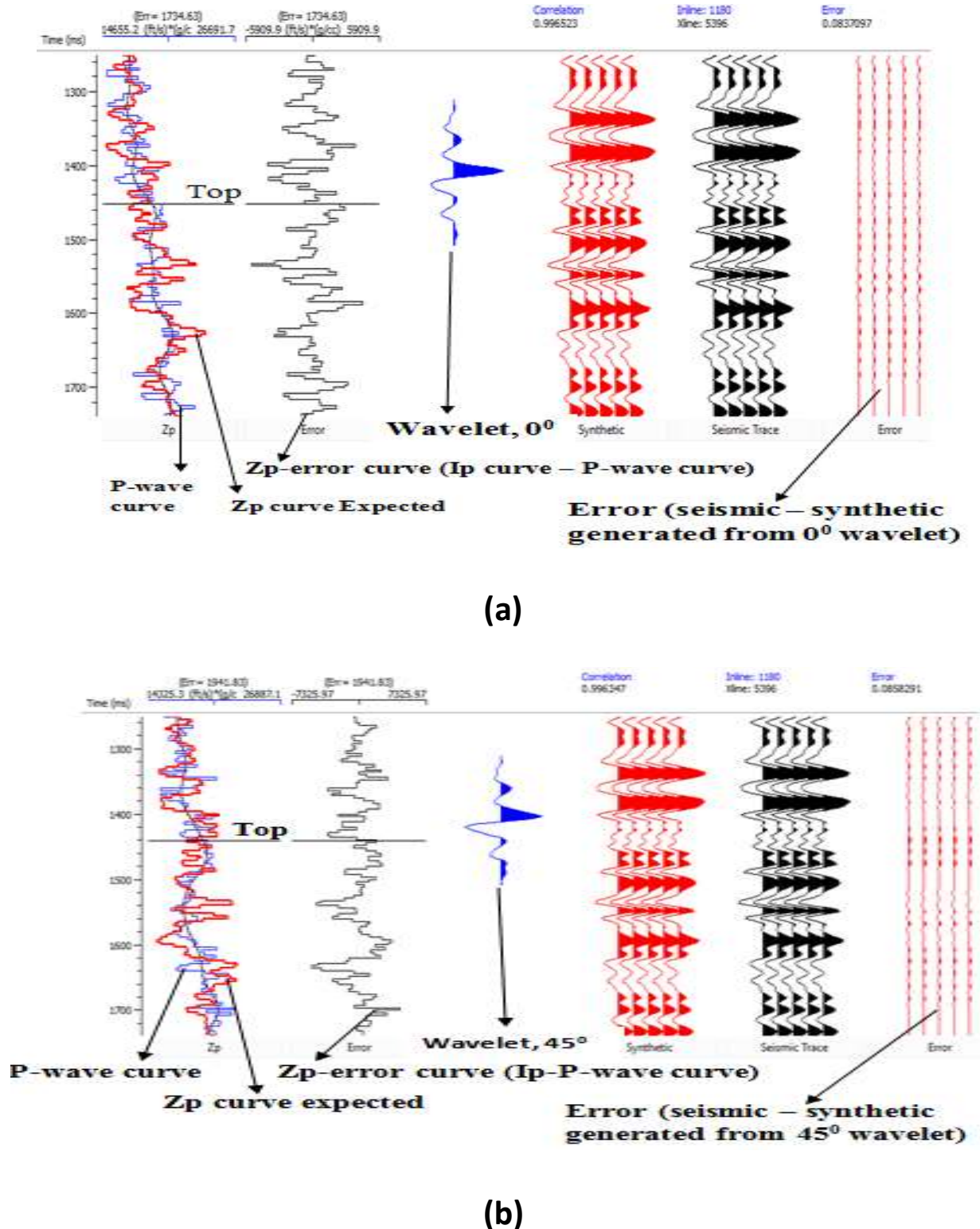
(a)

(b)

Figure 6. Show the expected Zp curves (red) and its errors (black) with coefficients calculated from seismic and synthetic traces from (a) 0° and and (b) 45° wavelet phases respectively.

1.5357 to 1.7000 ×10⁴ m/s × g/cc in red corresponds to probable sandstone lithology. This delineated sand lithology is dominant in the study area as deciphered in the inverted section. Away from the reservoir top, shows

Table 1. Impedance and synthetic errors with different wavelet phases.

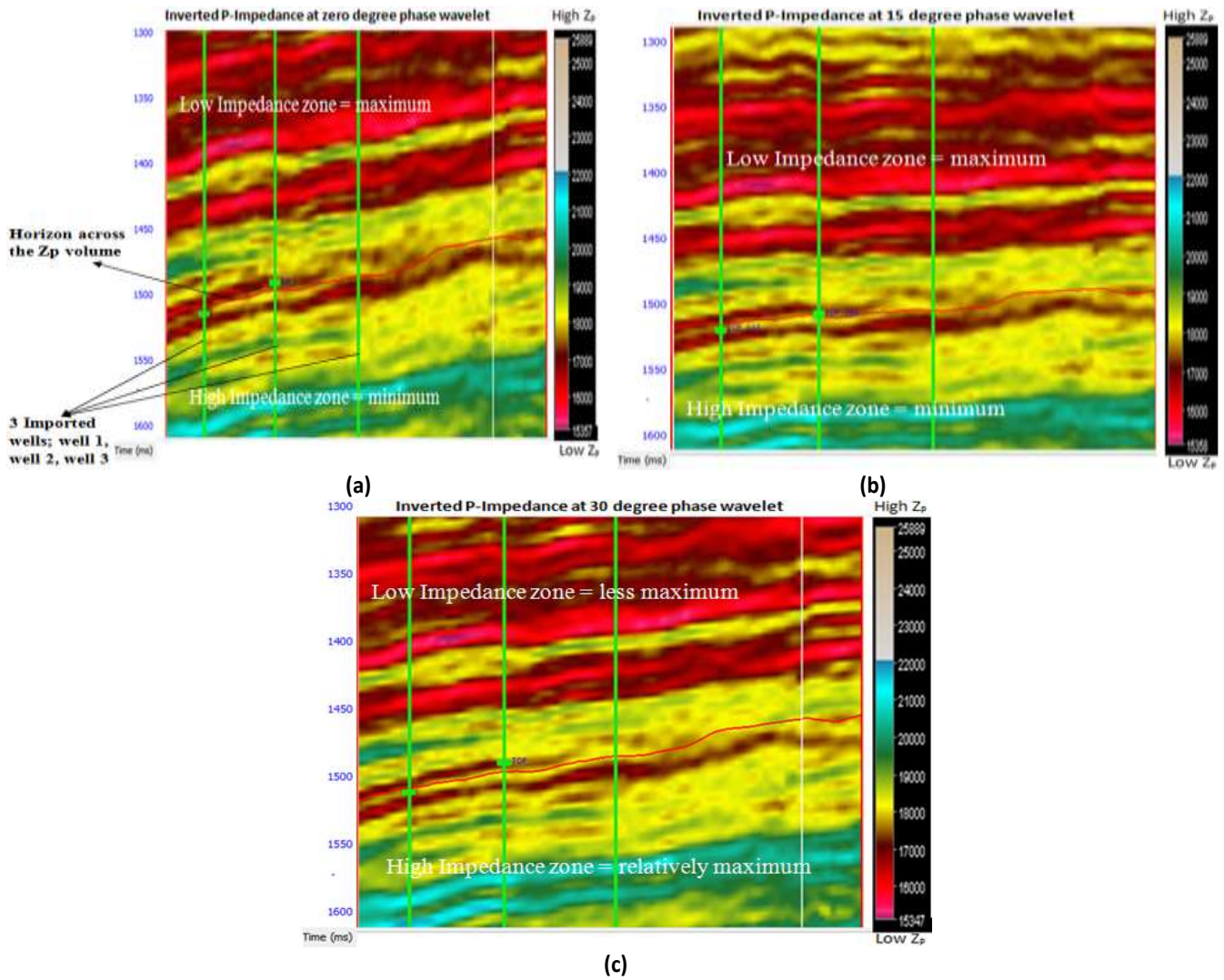| Wavelet phase (°)	P-Impedance error	Correlation coefficient	Synthetic error
0	1734.63	0.996523	0.0837097
15	1828.1	0.996412	0.0850209
30	1888.29	0.996372	0.0855129
45	1941.83	0.996347	0.0858291
60	1989.95	0.99634	0.0859302

Figure 7. P-Impedance (Z_P) distributions by (a) 0° (b) 15° and (c) 30° wavelet phase with picked horizon across the top of reservoir of three wells imported.

intermediate acoustic impedance values ranging from 1.8000 to 2.2000 $\times 10^4$ m/s × g/cc in yellow and cyan colour. These zones correspond to wet sands which could be saturated with brine. The highest I_P values ranging from 2.3000 to 2.5889 × 10^4 m/s × g/cc in grey colour are the shale beds. These areas are totally obscured for the 0, 15 and 30° phase wavelet inverted sections.

Figure 8(a) and (b) shows the inverted P-impedance cross-section for the 45 and 60° wavelet phase from a time window of 1300-1600 ms. The inverted sections for these two wavelets reveal an entirely poor match between
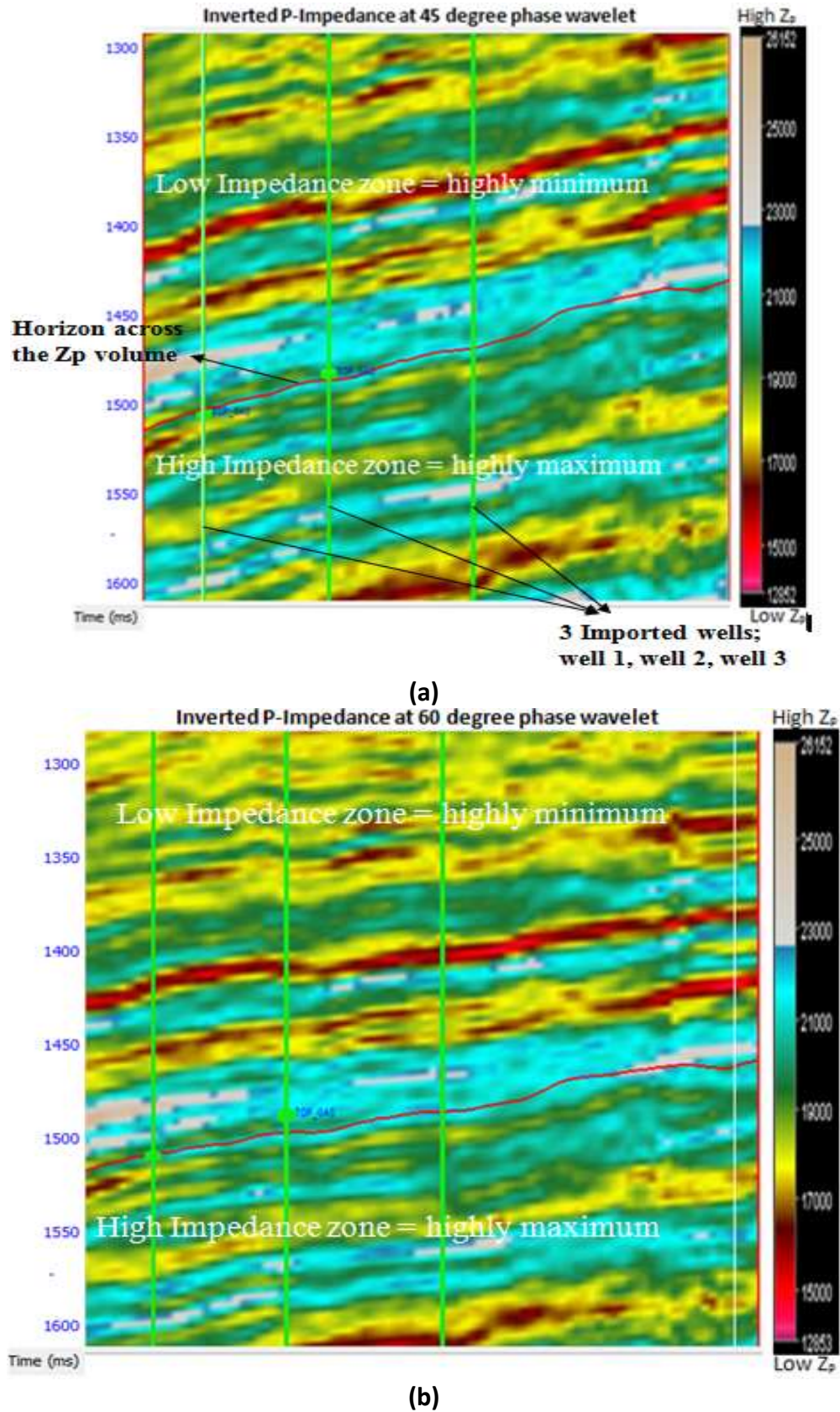
(a)

(b)

Figure 8. P-Impedance (Z_P) distributions by (a) 45° and (b) 60° wavelet phase with picked horizon across the top of reservoir of three wells imported.

the inverted sections and the picked horizon. An entirely opposite relationship is deciphered in the match between the I_P features distribution as compared to the inverted sections obtained using the 0, 15 and 30° acoustic impedance crosssections. The low and high impedance obviously disagrees at the reservoir tops as seen through the horizon across the inverted sections. At the reservoir top, around a time window of 1500 ms, the lowest I_P values range from $1.2852 - 1.7000 \times 10^4$ m/s × g/cc in red which correspond to probable sandstone lithology. The section reveals that the area has very little sandstone deposition. Also, away from the reservoir top, the intermediate acoustic impedance values of $1.7000-2.1000 \times 10^4$ m/s × g/cc is observed in yellow and cyan which correspond to wet sands. Meanwhile, the highest I_P values of $2.3000 - 2.6152 \times 10^4$ m/s × g/cc is observed in grey colour which is relatively high around the well locations indicating shale zones.

DISCUSSION

From literature findings, wavelet remains a link to seismic inversion in which the underlying geologic structure responsible for a seismic spike is extracted to better define the seismic response. But then, no two wavelets with different phases build the same initial impedance model. As such, the type of wavelet phases either zero phase/minimum phase greatly influence the initial geologic background and hence the P-impedance volume. However, the effects of wavelet phases on post stack inversion are deciphered through the nature of the different P-impedance results and their corresponding inverted and synthetic errors as summarized in Table 1.

When zero degree phase wavelet is used for inversion, the results obtained follow almost the same trend as the well data which is an indication of a good inversion result. Also, employing 15 and not more than 30° wavelet phase for inversion produces an inverted result which agrees with the study area geology. However, when wavelet with phase greater than 30° is considered, the inversion result is seen to disagree with the geology of the area. For instance, low impedance region depicts high impedance while areas with intermediate impedance become extremely high as deciphered in Figure 7. For the case of 45 and 60° phases, the inversion results show a relatively high impedance layer within the low impedance layer across the top of the reservoir indicated by the picked horizon.

From Table 1, it is noted that wavelet phases have a significant influence on the post stack inversion result thereby making the seismic inversion a non-reliable or a unique solution in litho-fluid discrimination. For instance, a zero phase wavelet or minimum phase (15°) has relatively small decrease in P-impedance error, increase in correlation and corresponding decrease in synthetic error. Comparing this with result of 45 and 60° wavelet phases, impedance error increases with a corresponding

increase in synthetic error but relatively small decrease in correlation coefficients.

Conclusion

The influence of seismic wavelet phase rotation in X-field revealed that zero phase or minimum phase wavelets are the most desirable for interpretation purpose. The results reveal that the degree of variation in phase of the input wavelet greatly affects the inversion with higher phase shift corresponding to higher error in impedance result. Most importantly, zero phase wavelet or minimum of 15° and not more than 30° follows the geology of the study area and is thus recommended as the right wavelet reliable for post stack inversion.

CONFLICT OF INTERESTS

The authors have not declared any conflict of interests.

ACKNOWLEDGEMENTS

REFERENCES

Ajaegwu NE, Odoh BI, Akpunomu EO, Obiadi I, Anakwuba EK (2012). Late Miocene to Early Pliocene Palynostratigraphy and Paleoenvironments of ANE-1 Well, Eastern Niger Delta. Nigeria. Journal of Mining and Geology 48:31-43.
Alaminiokuma GI, Ofuyah WN (2017). Time-lapse Seismic Acquisition in the Niger Delta: Challenges and Successes. Geosciences7:7-19.
Chirag J (2013). Effect of Seismic wavelet phase on post stack inversion. 10th Biennial International Conference & Exposition.
Doust H, Omatsola E (1990). Passive margin basins; Tulsa. American Association of Petroleum Geologists memoir 48:239-248.
Downtown JE (2005). Seismic parameter estimation from AVO inversion. Ph.D Thesis, University of Calgary, Alberta.
Gluck S, Deschizeaux B, Mignot AP, Huguet F (2000). Time-lapse impedance inversion of post-stack seismic data. Expanded abstracts, 70th Annual Meeting SEG, Calgary, 1509-1512.
Latimer RB, Davidson R, Van-Riel P (2000). An interpreter's guide to understanding and working with seismic-derived acoustic impedance data. The Leading Edge 19(3):242-256.
Margrave GF, Lawton DC, Stewart RR (1998). Interpreting channel sands with 3c-3d seismic data. The Leading Edge 17:509-513.
Maurya PS, Sarkar P (2016). Comparison of Post-Stack Seismic Inversion Methods: A case study of Blackfoot Field, Canada. International Journal of Scientific and Engineering Research 7:1091-1101.
Michele LW, Ronald RC, Michael EB (1999). The Niger Delta Petroleum System: Niger Delta Province, Nigeria, Cameroun and Equatorial Guinea, Africa. USGS Open files report, pp. 99-118.
Nuhu GO (2009). Geology and mineral resources of Nigeria. Springer Dordrecht, New York.
Oldenziel T (2003). Time lapse seismic within reservoir engineering Ph.D Thesis, Delft University of Technology.

Reijers TJ (1996). Stratigraphy and sedimentation of Niger Delta. Geologos 17:136-158.

Short C, Stauble A (1967). Outline of the geology of Niger Delta. Association of Petroleum Geologist Bulletin 54:761-779.

Van-Riel P (2000). The past, present and future of reservoir characterization. The Leading Edge 19 :878-881.

Veeken PC, Rauch-Davies M (2006). AVO Attribute analysis and seismic reservoir characterization. First Break 24:41-52.

Weber KJ, Daukoru E (1975). Petroleum Geology of the Niger Delta. Tokyo 9th World Petroleum Congress Proceedings 2:209-2011.